Flood, R.D., Piper, D.J.W., Klaus, A., and Peterson, L.C. (Eds.), 1997
Proceedings of the Ocean Drilling Program, Scientific Results, Vol. 155

15. *DATA REPORT*: BETWEEN-HOLE CORRELATIONS OF SITES DRILLED DURING LEG 155 ON THE AMAZON FAN[1]

Frank R. Hall[2]

ABSTRACT

Seventeen sites were drilled during Ocean Drilling Program Leg 155 on the Amazon Fan. Of these 17 sites, 11 have multiple holes. A correlation scheme for seven of these holes is presented using the whole-core magnetic susceptibility records collected during the cruise.

INTRODUCTION

This data report discusses the whole-core magnetic susceptibility records for Leg 155 (Fig. 1) that were used as a between-hole correlation tool for sites that had multiple holes (e.g., Robinson, 1990). The methods used to collect these data are reported in Flood, Piper, Klaus, et al. (1995).

Of the 17 sites drilled, 11 had two or more holes. Seven of these 11 sites provided records that could be correlated using the whole-core susceptibility data (Table 1). Data from Sites 931, 936, 941, and 944 were not included in these analyses as it was not possible to correlate these particular records.

METHODS

Prior to correlation, anomalous data values were removed. These data typically occurred at section breaks or were considered associated with gas voids in the cores. In addition, the downhole trends associated with compaction were removed from individual data sets by linear regression, and the data were smoothed using a five-point running mean.

Correlations were attempted by comparing the individual peaks and troughs of the records. In addition, data provided by the locations of lithologic unit and subunit boundaries were used to constrain the tie points. The data were plotted with respect to the depths given in the shipboard logs. They were not adjusted with respect to any particular hole.

RESULTS AND DISCUSSION

The data are presented in both graphical and tabular form. Table 2 gives the downhole depths of the tie points for each hole. Figures 2 through 8 show the locations of the tie points with respect to the data curves and locations of core boundaries, whereas Figures 9 and 10 show the depth-depth plots of the tie points for each site. Tie points with a higher degree of uncertainty have a question mark (?) next to them. In addition, depth-depth plots are included with the figures. If more than two holes were correlated, the depths of the other holes were plotted against the most complete hole.

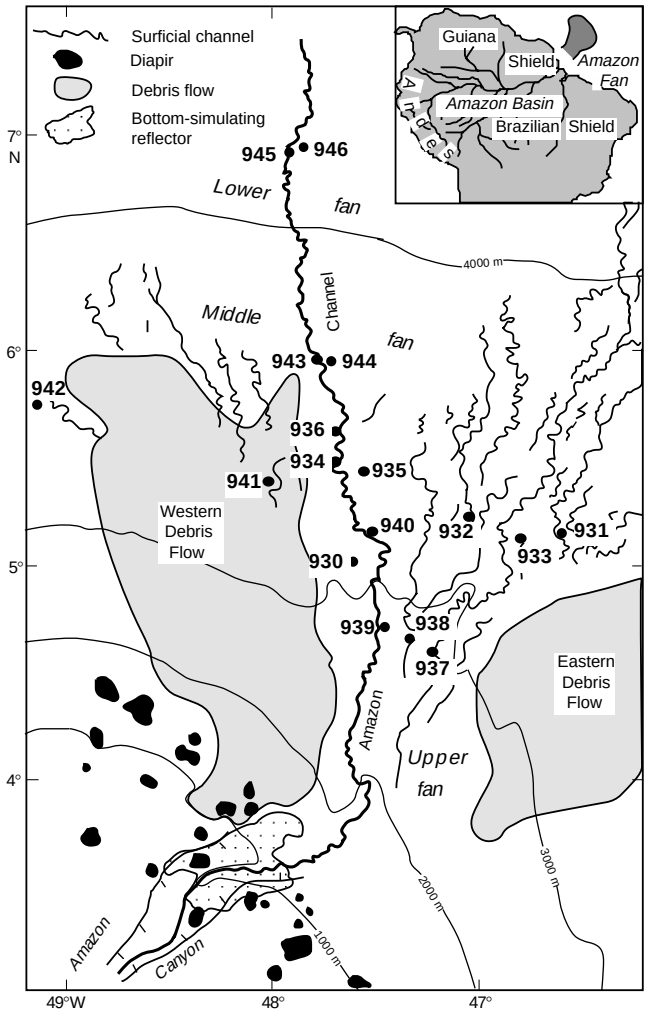

Figure 1. The location of the Amazon Fan and all sites occupied during Leg 155. From Flood et al., 1995; modified from Damuth et al., 1988, and Manley and Flood, 1988.

[1]Flood, R.D., Piper, D.J.W., Klaus, A., and Peterson, L.C. (Eds.), 1997. *Proc. ODP, Sci. Results*, 155: College Station, TX (Ocean Drilling Program).

[2]Graduate College of Marine Studies, University of Delaware, Newark, DE 19716, U.S.A. frhall@udel.edu

Previous Chapter | Table of Contents | Next Chapter

Table 1. Locations of sites used in this study.

Site	Latitude (north)	Longitude (west)	Water depth (m)
930	5°00′73″	47°35′63″	3128
932	5°12′79″	47°02′06″	3384
934	5°29′04″	47°40′87″	3415
937	4°35′17″	47°11′51″	2797
938	4°39′60″	47°18′82″	2811
939	4°43′36″	47°30′22″	2794
942	5°44′24″	49°07′39″	3368

Site 937

Two holes are included in the correlation for Site 937: Holes 937B and 937C (Hole 937A is <1 m long). Ten potential tie points (Fig. 5; *a*–*j*) were recognized. Because the signal gets noisier below point *e*, the remaining tie points are less certain.

Site 938

Two holes are included in the correlations: Holes 938A and 938B. Thirteen potential tie points (Fig. 6; *a*–*m*) were recognized. Cores 155-938A-7H and 155-938A-8H were considered to be disturbed. Therefore, the tie points below point *i* are less certain.

Site 939

Two holes were included in this correlation: Holes 939A and 939B. Fourteen potential tie points (Fig. 7; *a*–*n*) were recognized. Point *n* is located near the end of Core 155-939B-10H. Point *n* is therefore considered uncertain.

Site 942

Three holes were included in the correlation of Site 942: Holes 942A, 942B, and 942C. Sixteen potential tie points between holes (Fig. 8; *a*–*p*) were recognized. Only Hole 942A appears to have a complete sequence. This is because of poor recovery of Cores 155-942B-5H and 6H. Furthermore, large gaps in the record occur between cores 155-942C-2H and 3H and also between Cores 155-942C-4H and 5H.

CONCLUSION

Whole-core magnetic susceptibility records were used to correlate between holes at seven sites occupied during Leg 155. Other data sets, especially age control via ^{14}C dates, will be necessary to refine the between-site correlations in the future.

ACKNOWLEDGMENTS

I thank the co-chief scientists of this cruise (Drs. Roger Flood and David Piper), Dr. Stanley Cisowski, and an anonymous reviewer for comments to this text. This research was supported by USSSAC grant No. 155-20846b.

REFERENCES

Damuth, J.E., Flood, R.D., Kowsmann, R.O., Belderson, R.H., and Gorini, M.A., 1988. Anatomy and growth pattern of Amazon deep-sea fan as revealed by long-range side-scan sonar (GLORIA) and high-resolution seismic studies. *AAPG Bull.*, 72:885–911.

Flood, R.D., Piper, D.J.W., Klaus, A., et al., 1995. *Proc. ODP, Init. Repts.*, 155: College Station, TX (Ocean Drilling Program).

Flood, R.D., Piper, D.J.W., and Shipboard Scientific Party, 1995. Introduction. *In* Flood, R.D., Piper, D.J.W., Klaus, A., et al., *Proc. ODP, Init. Repts.*, 155: College Station, TX (Ocean Drilling Program), 5–16.

Manley, P.L., and Flood, R.D., 1988. Cyclic sediment deposition within Amazon deep-sea fan. *AAPG Bull.*, 72:912–925.

Robinson, S.G., 1990. Applications for whole-core magnetic susceptibility measurements of deep-sea sediments: Leg 115 results. *In* Duncan, R.A., Backman, J., Peterson, L.C., et al., *Proc. ODP, Sci. Results*, 115: College Station, TX (Ocean Drilling Program), 737–771.

Date of initial receipt: 1 December 1995
Date of acceptance: 7 May 1996
Ms 155SR-252

Table 2. Depths of tie points of all sites.

	930B		930D		930C	
Tie point	Depth (mbsf)	Core, section	Depth (mbsf)	Core, section	Depth (mbsf)	Core, section
a	12.05	2H-5, 35	6.17	2H-2, 67		
b	12.74	2H-5, 105	8.22	2H-3, 122		
c	30.09	4H-4, 89	38.29	5H-4, 129		
d	46.09	6H-2, 89	44.44	6H-2, 94	49.79	1H-1, 76
e	59.84	7H-5, 64			65.14	4H-6, 14
f	94.29	11H-3, 9			92.74	7H-5, 74
g	114.1	13X-3, 89			118.4	10X-3, 70
h	129.1	14X-7, 129			128.4	11X-3, 139
i	198.2	22X-2, 30			203.9	13X-2, 129

	932A		932B	
Tie point	Depth (mbsf)	Core, section	Depth (mbsf)	Core, section
a	2.03	1H-2, 53	1.89	1H-2, 39
b	4.8	1H-1, 30	4.3	1H-3, 130
c	6.98	2H-1, 98	5.99	2H-1, 99
d	11.01	2H-4, 51	10.69	2H-4, 119
e	12.62	2H-5, 62	11.69	2H-5, 69
f	16.21	3H-1, 71	15.14	3H-1, 64
g	18.64	3H-3, 14	17.65	3H-3, 15
h	20.63	3H-4, 63	19.54	3H-4, 54
i	24.22	3H-6, 122	24.44	4H-1, 44
j	30.36	4H-4, 86	28.54	4H-4, 4
k	34.45	4H-7, 45	33.39	4H-7, 39
l	40.54	5H-5, 4	37.74	5H-3, 125
m	43.19	5H-6, 119	40.14	5H-5, 64
n	43.99	5H-7, 49	41.24	5H-6, 25
o	46.59	6H-2, 109	45.49	6H-2, 99

	934A		934B	
Tie point	Depth (mbsf)	Core, section	Depth (mbsf)	Core, section
a	0.52	1H-1, 52	0.55	1H-1, 55
b	3.88	1H-3, 88	5.89	1H-4, 139
c	5.27	2H-1, 97	6.86	1H-5, 86
d	7.61	2H-3, 31	8.57	2H-1, 107
e	12.36	2H-6, 56	12.86	2H-4, 86
f	14.29	3H-1, 49	15.61	2H-6, 62
g	18.74	3H-4, 45	18.8	3H-1, 130
h	22.35	3H-6, 105	22.4	3H-4, 40
i	27.19	4H-3, 89	27.94	4H-1, 140
j	28.74	4H-4, 94	30.25	4H-1, 75
k	30.9	4H-6, 10	32.1	4H-5, 29
?			35.69	4H-1, 94
l	35.19	5H-2, 89	37.55	5H-2, 5
m	37.54	5H-4, 25	38.94	5H-2, 144

	937B		937C	
Tie point	Depth (mbsf)	Core, section	Depth (mbsf)	Core, section
a	1.66	1H-2, -16	1.64	1H-2, 14
b	5.56	1H-4, 106	6.24	1H-5, 24
c	14.5	2H-5, 100	14.1	2H-4, 60
d	23.69	3H-5, 69	22.09	3H-3, 59
e	36.34	5H-1, 34	40.69	5H-3, 19
f	47.63	6H-2, 95	51.34	6H-3, 134
g	52.07	6H-1, 89	55.09	6H-6, 59
h	65.32	8H-2, 34	64.96	7H-6, 104
i	69.01	8H-4, 119	67.89	8H-2, 39
j	71.01	8H-6, 19	69.34	8H-3, 34

	938A		938B	
Tie point	Depth (mbsf)	Core, section	Depth (mbsf)	Core, section
a	4.24	1H-3, 125	4.89	1H-4, 40
b	10.55	2H-2, 145	13.84	2H-6, 104
c	20.2	3H-3, 10	20.04	3H-4, 74
d	24.02	3H-5, 92	24.87	4H-2, 24
e	25.99	3H-6, 139	27.02	4H-3, 89
f	30.85	4H-4, 84	30.16	4H-5, 109
g	35.8	4H-7, 129	34.54	5H-1, 74
h	44.95	5H-7, 5	47.29	6H-3, 125
i	48.98	6H-4, 14	48.74	6H-5, 59
j?	67.35	8H-2, 125	65.69	8H-4, 115
k?	71.09	8H-5, 64	71.94	9H-1, 14
l?	79.73	9H-1, 110	78.55	9H-5, 75
m?	80.38	9H-6, 25	78.8	9H-5, 100

	939A		939B		939C	
Tie point	Depth (mbsf)	Core, section	Depth (mbsf)	Core, section	Depth (mbsf)	Core, section
a	9	2H-1, 130	7.64	2H-3, 65	7.3	1H-5, 130
b	20.71	3H-4, 30	15.93	3H-3, 59	17.3	3H-1, 20
c	24.44	3H-7, 30	19.39	3H-5, 105	19.84	3H-3, 19
d	40.99	5H-4, 30	33.34	5H-1, 84	28.5	4H-3, 40
e	44.44	5H-6, 34	36.24	5H-3, 74	31.14	4H-4, 4
f	56.1	7H-1, 90	45.6	6H-4, 39		
g	59.77	7H-5, 24	48.35	6H-6, 14		
h	64.94	8H-1, 24	52.16	7H-2, 49		
i	67.29	8H-2, 134	53.91	7H-3, 74		
j	70.09	8H-4, 114	59.36	7H-7, 20		
k	79.57	9H-4, 94	64.7	8H-4, 125		
l	82.88	9H-6, 125	67.09	8H-6, 65		
m	89.4	10X-4, 120	76.7	9H-5, 115		
n?	95.39	11X-2, 69	87.14	10X-5, 115		

	942A		942B		942C	
Tie point	Depth (mbsf)	Core, section	Depth (mbsf)	Core, section	Depth (mbsf)	Core, section
a	3.37	1H-3, 37	4.1	1H-3, 110	3.43	1H-3, 44
b	9.21	2H-4, 91	9.7	2H-2, 70	4.8	2H-1, 50
c	13.88	3H-1, 58	14.64	2H-5, 114	9.53	2H-4, 73
d	15.05	3H-2, 25	15.74	2H-6, 74	10.76	2H-5, 46
e	17	3H-3, 70	18.25	3H-1, 125		
f	23.84	4H-1, 104	24.25	3H-5, 125		
g	27.69	4H-4, 59	27.15	4H-1, 65		
h	32.69	5H-1, 39	32.19	4H-4, 119		
i	43.44	6H-2, 14			40.59	3H-4, 9
j	53.19	7H-2, 39			50.19	4H-4, 19
k	55.74	7H-3, 144	56.79	7H-2, 30	53.09	4H-6, 9
l	60.45	7H-7, 15	61.3	7H-5, 30	54.8	4H-7, 30
m	65.84	8H-4, 54	65.29	8H-1, 80	62.19	5H-1, 20
n	66.85	8H-5, 5	67.1	8H-1, 110	64.5	5H-2, 100
o	69.59	8H-6 129	69.64	8H-4, 65	66.37	5H-4, 14
p	71.19	9H-1, 89	71.14	8H-5, 64	68.74	5H-6, 55

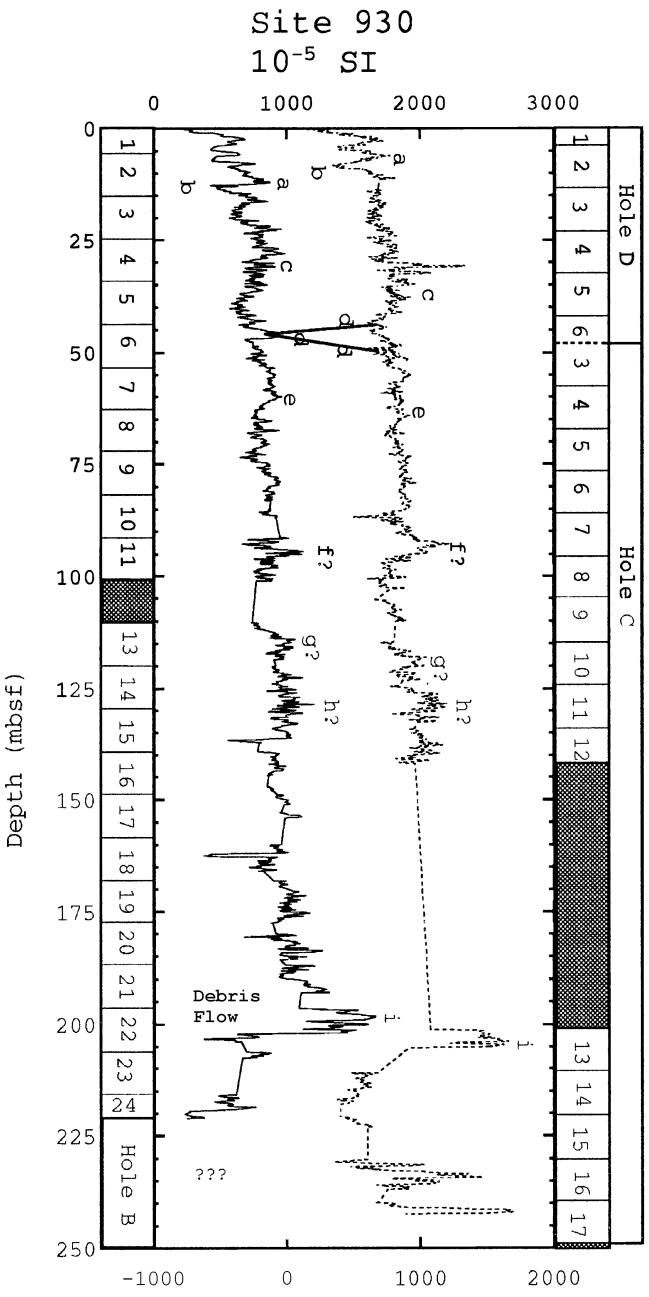

Figure 2. The whole-core magnetic susceptibility plots for Site 930.

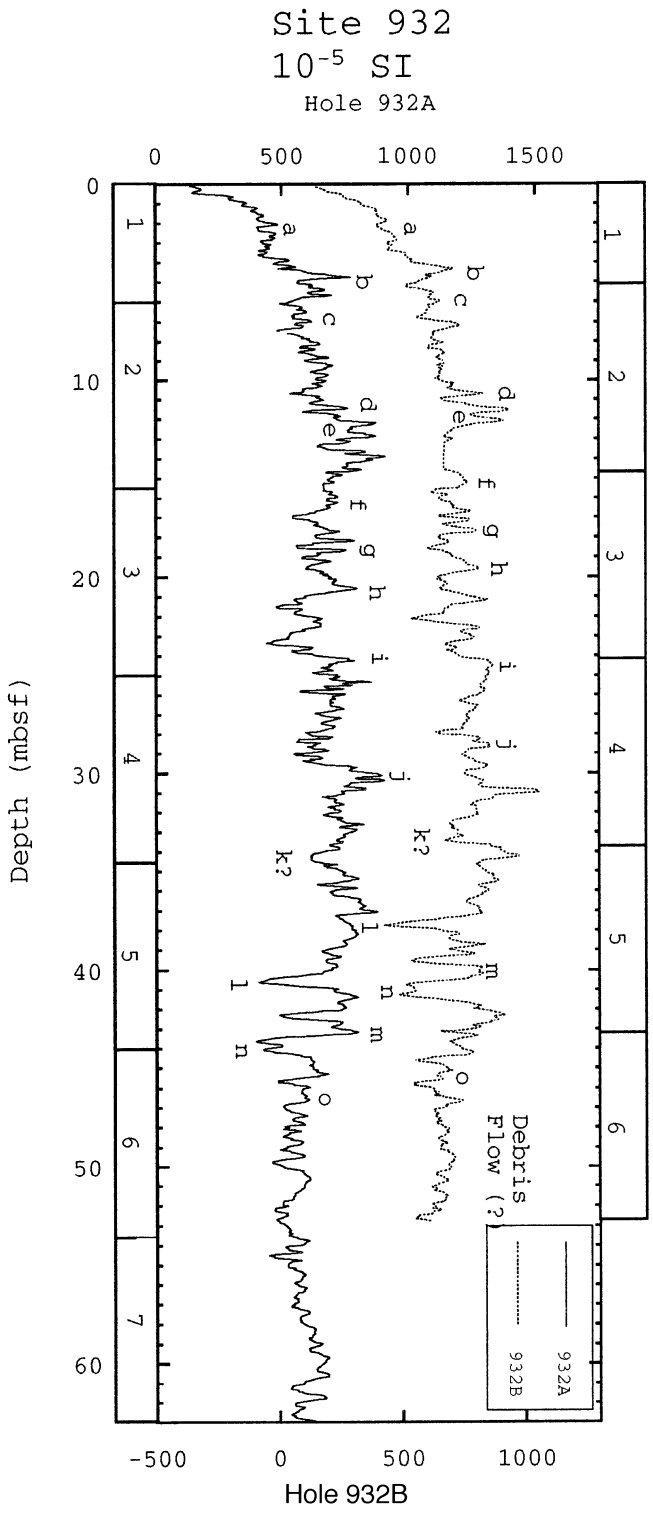

Figure 3. The whole-core magnetic susceptibility plots for Site 932.

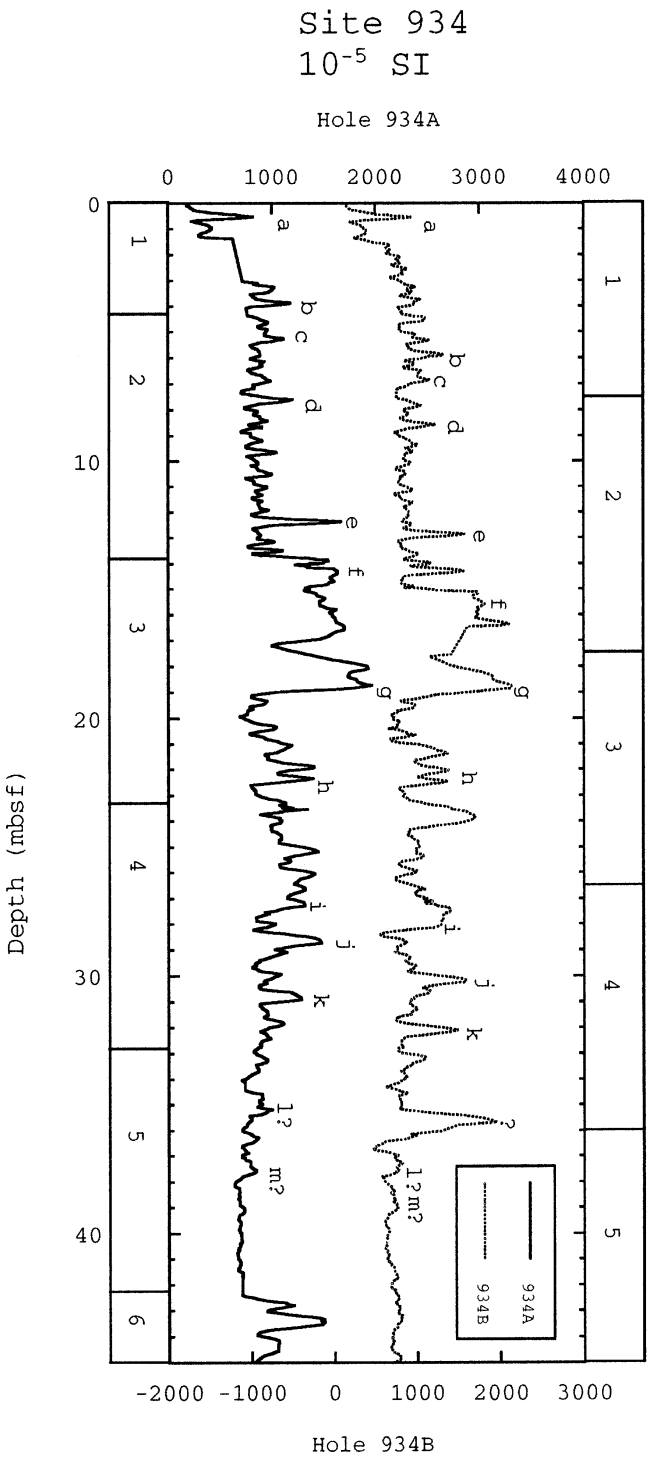

Figure 4. The whole-core magnetic susceptibility plots for Site 934.

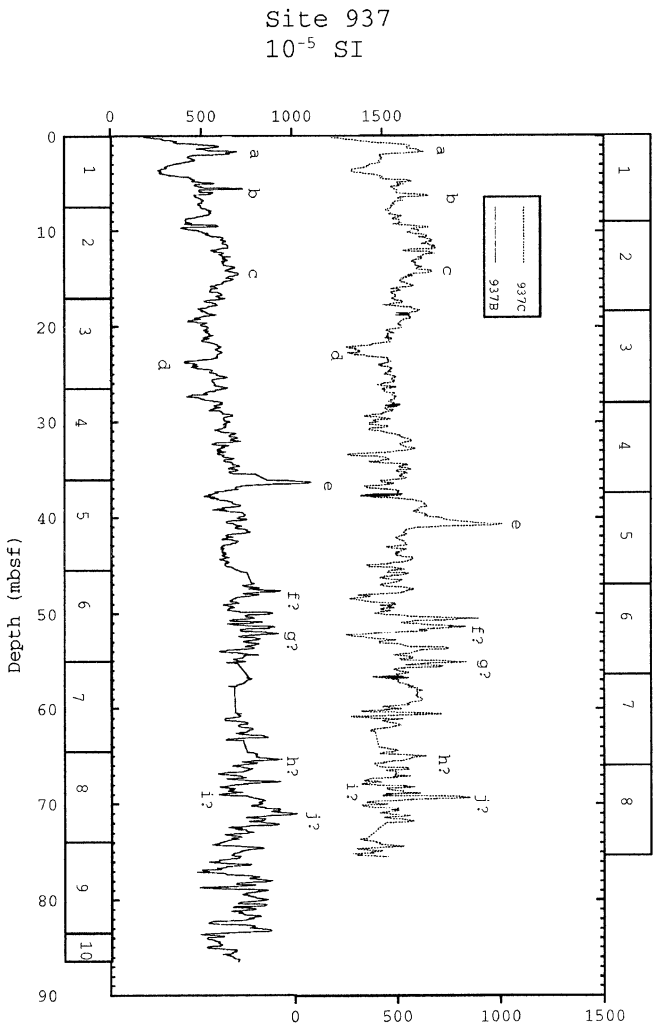

Figure 5. The whole-core magnetic susceptibility plots for Site 937.

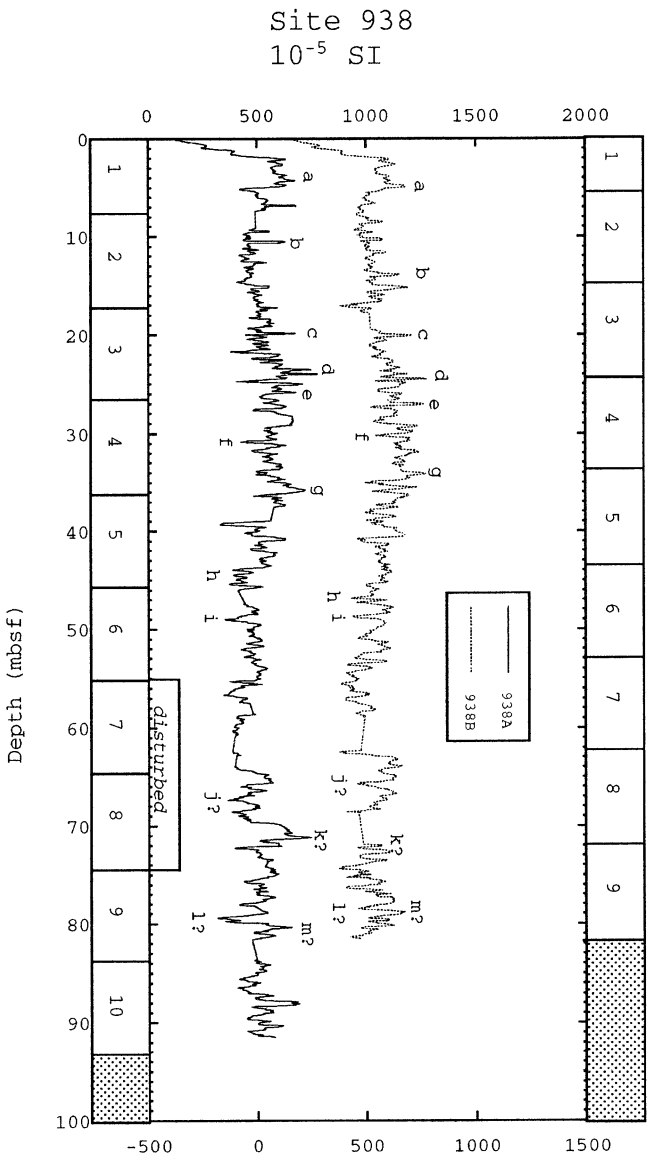

Figure 6. The whole-core magnetic susceptibility plots for Site 938.

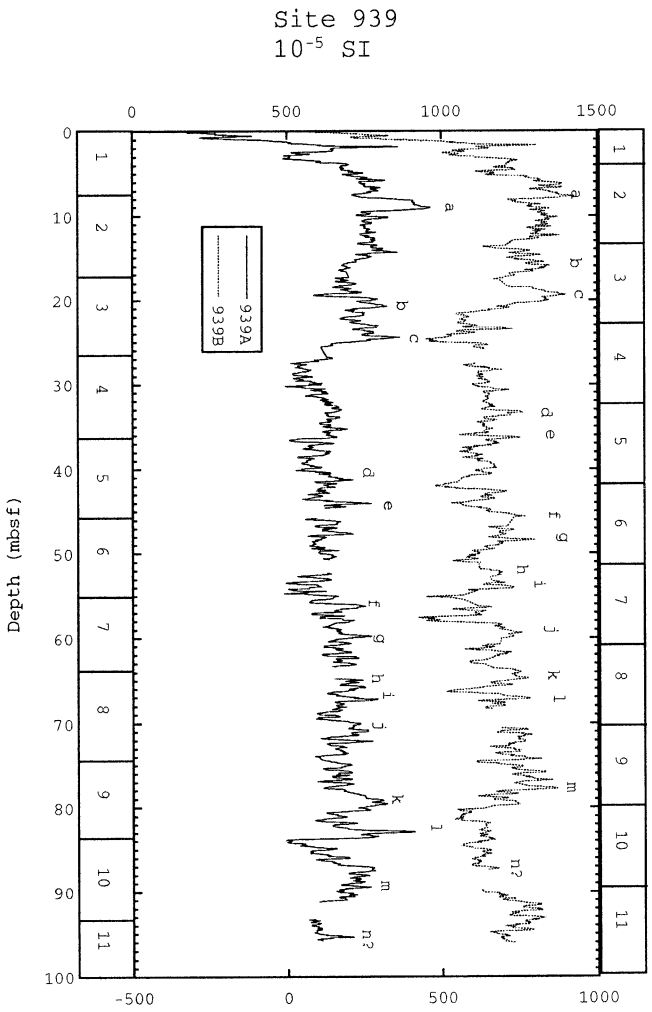

Figure 7. The whole-core magnetic susceptibility plots for Site 939.

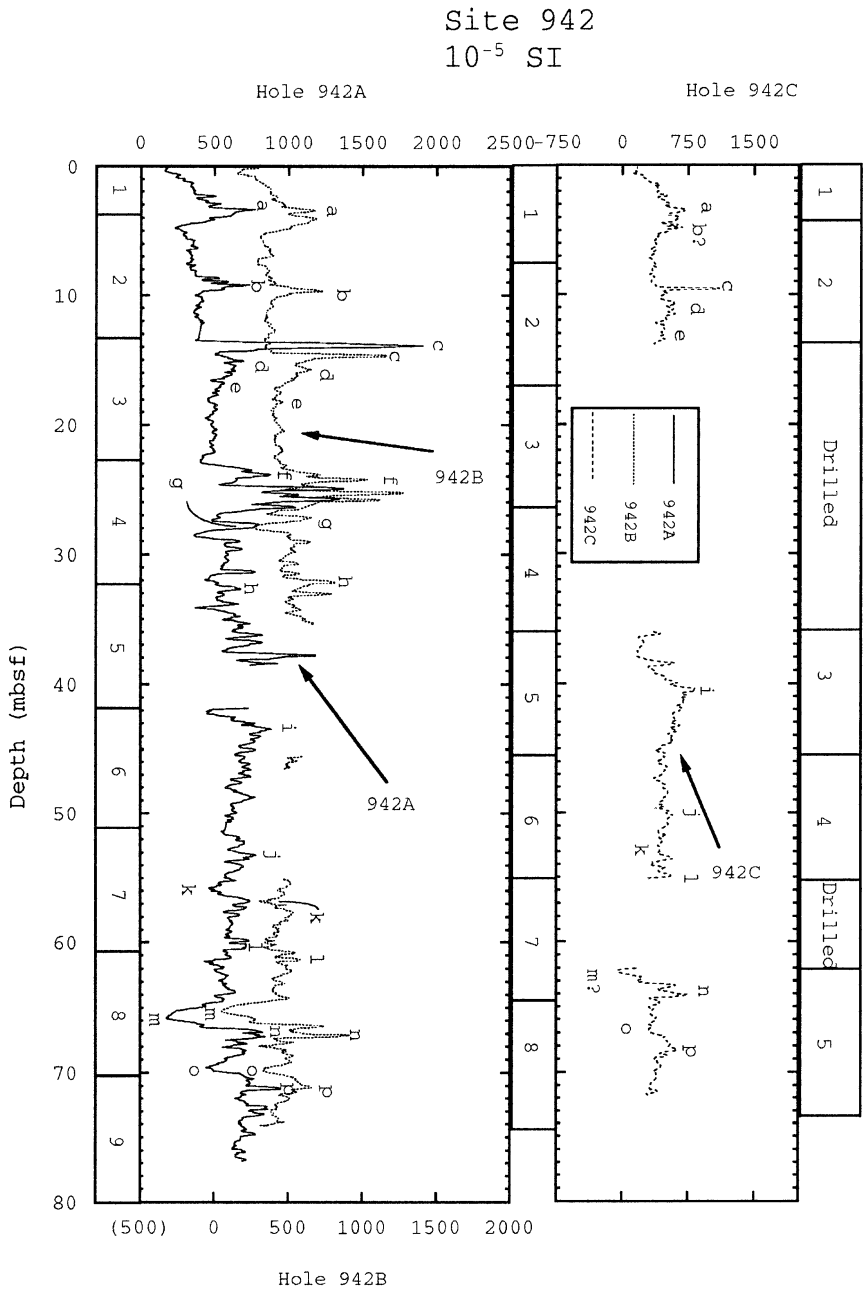

Figure 8. The whole-core magnetic susceptibility plots for Site 942.

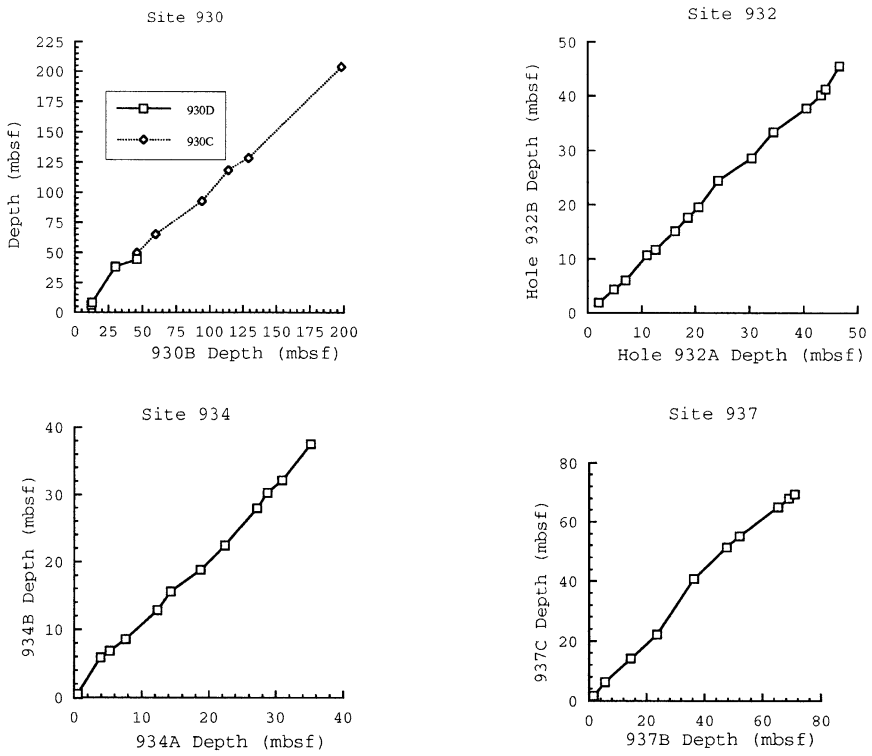

Figure 9. The depth-depth plots for the tie points for Sites 930, 932, 934, and 937.

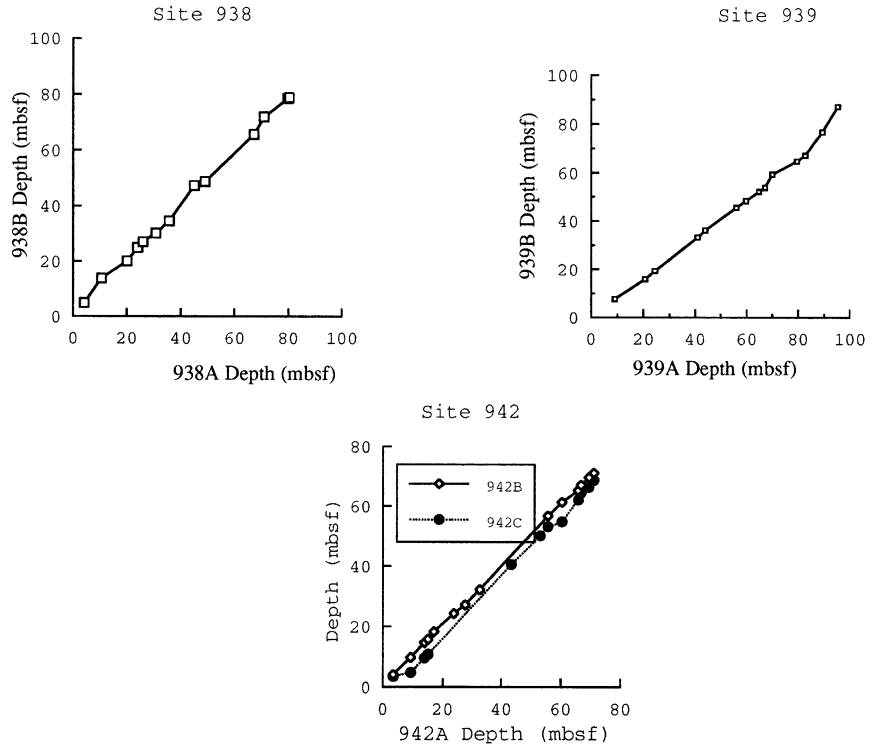

Figure 10. The depth-depth plots for the tie points for Sites 938, 939, and 942.

Previous Chapter Table of Contents Next Chapter